Table I. Half-Wave Potentials (V vs. SCE) and Spectral Characteristics of Investigated Compounds in Acetonitrile[a]

compd	$E_{1/2}(1)$	$\Delta E_{1/2}$, V	$E_{1/2}(2)$	$\Delta E_{1/2}$, V	λ_{max}, nm ($10^{-2}\epsilon$, M^{-1})	
$Rh_2(ac)_4$ (I)	1.17	0.26			551 (2.7)	437 (1.9)
$Rh_2(ac)_3(acam)$ (II)	0.91	0.29			542 (2.2)	416 (1.7)
$Rh_2(ac)_2(acam)_2$ (III)	0.62	0.25			528 (2.0)	398 (sh), 359 (sh)
$Rh_2(ac)(acam)_3$ (IV)	0.37	0.22	1.65	0.24	514 (2.0)	356 (sh)
$Rh_2(acam)_4$ (V)	0.15		1.41		500 (2.2)	345 (sh)

[a] Half-wave potentials are measured in the presence of 0.1 M TBAP. sh = shoulder.

present with any of the other four complexes. This extra shoulder may be due to one of the three unresolved isomers, or it may be that compound III is spectrally more complex than any of the other complexes.

In summary, the experimental fact that $Rh_2(ac)_n(acam)_{4-n}$ has spectral and electrochemical properties between those of $Rh_2(ac)_4$ and $Rh_2(acam)_4$ should provide a basis for systematically examining the Rh_2^{4+}, Rh_2^{5+}, and Rh_2^{6+} units as a function of controlled changes in the bridging ligand. Literally hundreds of different combinations of R, R′, and R″ may be utilized in the synthesis of novel $Rh_2(RONCR')_n(O_2CR'')_{4-n}$ complexes. Thus, a carefully designed synthetic series of dirhodium(II) compounds can be used to systematically probe the electronic levels of the metal–metal bond in the oxidized and reduced species. This degree of structural control has never been available before and should provide the basis for a much better understanding of structure–reactivity relationships with these type compounds.

Acknowledgment. The support of the Robert A. Welch Foundation (K.M.K., Grant E-680; J.L.B, Grant E-918) is gratefully acknowledged.

Registry No. I, 15956-28-2; II, 87985-37-3; II (monooxidized), 87985-41-9; III, 87985-38-4; III (monooxidized), 87985-42-0; IV, 87985-39-5; IV (monooxidized), 87985-43-1; IV (dioxidized), 87985-45-3; V, 87985-40-8; V (monooxidized), 87985-44-2; V (dioxidized), 87985-46-4.

Department of Chemistry
University of Houston
Houston, Texas 77004

T. P. Zhu
M. Q. Ahsan
T. Malinski
K. M. Kadish*
J. L. Bear*

Received September 30, 1983

Articles

Contribution from the Department of Chemistry,
The University of Texas at Austin, Austin, Texas 78712

Electrochemistry in Liquid Sulfur Dioxide. 5. Oxidation of Bipyridine and Phenanthroline Complexes of Osmium, Ruthenium, and Iron

JOHN G. GAUDIELLO, PAUL G. BRADLEY, KENNETH A. NORTON, WILLIAM H. WOODRUFF, and ALLEN J. BARD*

Received May 27, 1983

The electrochemical oxidation of bipyridine and phenanthroline complexes of Fe, Ru, and Os in liquid sulfur dioxide was investigated by cyclic voltammetry and coulometry. $Os(bpy)_3^{2+}$ and $Os(phen)_3^{2+}$ undergo two successive one-electron oxidations to form stable 3+ and 4+ species. In contrast $Fe(phen)_3^{2+}$ and $Ru(phen)_3^{2+}$, when oxidized to the 4+ form, produce an electroactive layer on the electrode surface. Electrochemical, magnetic susceptibility, and ^1H NMR data suggest that the oxidation to the 4+ form is metal centered in the Os complexes but ligand centered in the Fe and Ru complexes. Resonance Raman spectra of $Os(bpy)_3^{4+}$ exhibit unusual complexity that suggests either static inequivalency of the bpy ligands on the vibrational time scale or a multiple-minimum electronic potential.

Introduction

We showed in a previous study from our laboratory[1] that highly oxidized transition-metal complexes could be produced electrochemically in liquid sulfur dioxide. $Ru(bpy)_3^{2+}$ and $Fe(bpy)_3^{2+}$ (bpy = 2,2′-bipyridine) were oxidized in two successive one-electron oxidations to the 3+ and 4+ forms. The 3+ species were stable for hours while the 4+ species reacted with SO_2 in a catalytic cycle to regenerate the 3+ form. The 3+ → 4+ oxidation for $Ru(bpy)_3^{3+}$ and $Fe(bpy)_3^{3+}$ is believed to be ligand centered, on the basis of spectroscopic and electrochemical data.[1] We describe here the electrochemical oxidation of $Os(bpy)_3^{2+}$, $Fe(phen)_3^{2+}$, $Ru(phen)_3^{2+}$, and $Os(phen)_3^{2+}$ (phen = 1,10-phenanthroline) in liquid SO_2 along with information concerning the site of oxidation of the 3+ species. Both Os complexes form stable 3+ and 4+ forms while $Fe(phen)_3^{2+}$ and $Ru(phen)_3^{2+}$ undergo polymerization when oxidized to the 4+ species.

Magnetic susceptibility and ^1H NMR data are presented for the $Os(bpy)_3^{3+}$ and $Os(bpy)_3^{4+}$ species suggesting metal-centered oxidation. Resonance Raman (RR) spectroscopy of the series Os^{II}-, Os^{III}-, and $Os^{IV}(bpy)_3$ is also reported. The RR results are consistent with metal-centered oxidation in $Os(bpy)_3^{4+}$, if significant splitting of the ligand vibrational states occurs due to a dynamic Jahn–Teller effect or static ligand inequivalency.

Experimental Section

Measurements. Electrochemical measurements were made with a PAR Model 173 potentiostat, a Model 175 universal programmer, and a Model 179 digital coulometer (Princeton Applied Research

(1) Gaudiello, J. G.; Sharp, P. R.; Bard, A. J. *J. Am. Chem. Soc.* **1982**, *104*, 6373–6377.

0020-1669/84/1323-0003$01.50/0

Table I. Cyclic Voltammetry Data for Osmium 2,2'-Bipyridine and 1,10-Phenanthroline Complexes in Liquid Sulfur Dioxide[a]

	$Os(bpy)_3^{2+}$		$Os(bpy)_3^{3+}$		$Os(phen)_3^{2+}$		$Os(phen)_3^{3+}$	
scan rate, mV/s	$i_{pa}/v^{1/2}C^*A$, $\mu A\ s^{1/2}\ mM^{-1}\ cm^{-2}$	$E_{pa}-E_{pc}$, mV	$i_{pa}/v^{1/2}C^*A$, $\mu A\ s^{1/2}\ mM\ cm^{-2}$	$E_{pa}-E_{pc}$, mV	$i_{pa}/v^{1/2}C^*A$, $\mu A\ s^{1/2}\ mM\ cm^{-2}$	$E_{pa}-E_{pc}$, mV	$i_{pa}/v^{1/2}C^*A$, $\mu A\ s^{1/2}\ mM^{-1}\ cm^{-2}$	$E_{pa}-E_{pc}$, mV
10	420	47	460	48	360	48	340	46
20	420	45	470	46	370	46	330	48
50	410	46	460	47	370	45	330	47
100	420	46	460	47	360	47	330	45
200	410	48	460	45	370	48	320	45

[a] At −40 °C; 0.1 M $(TBA)BF_4$ as supporting electrolyte. Theoretical value of $E_{pa}-E_{pc}$ at −40 °C is 44 mV for one-electron Nernstian wave.

Corp., Princeton, NJ) employing positive feedback for *iR* compensation. A Model 2000 X-Y recorder (Houston Instruments Inc., Austin, TX) was used to record the current–voltage curves for scan rates less than 500 mV/s; for faster scan rates, a Norland digital oscilloscope, Model 3001 (Norland Corp., Fort Atkinson, WI), was used.

^1H NMR spectra were obtained at 200 MHz in the pulsed Fourier transform mode on a Nicolet NT-200 spectrometer at −60 °C. Chemical shifts in liquid SO_2 were measured and are reported relative to tetramethylammonium tetrafluoroborate ($(TMA)BF_4$) whose chemical shift is 2.5 ppm downfield from that of tetramethylsilane. Visible absorption spectra were obtained with a Model 1250 optical multichannel analyzer (Princeton Applied Research Corp., Princeton, NJ) in conjunction with a holographic grating (150 lines/mm) and a 150-W xenon lamp.

Materials. Tetra-*n*-butylammonium tetrafluoroborate ($(TBA)BF_4$) and $(TMA)BF_4$ were obtained commercially (Southwestern Analytical Chemicals, Austin, TX). $(TBA)BF_4$ was recrystallized three times from acetone/ether and dried in vacuo for 72 h. $(TMA)BF_4$ was used as received. 2,2'-Bipyridine, 1,10-phenanthroline, ruthenium trichloride, and osmium trichloride were purchased from Aldrich Chemical Co. and were used as received. All other chemicals were reagent grade.

Preparation of Complexes. $[Os(bpy)_3](PF_6)_2$ and $[Os(phen)_3](PF_6)_2$. $OsCl_3$ (275 mg, 0.93 mmol) and 6 equiv of the ligand were added to 50 mL of ethylene glycol and refluxed under nitrogen for 2 days. A 50-mL portion of H_2O was then added along with NH_4PF_6 to precipitate the PF_6^- salt. The resulting fine crystals were recrystallized three times from acetone/ether, washed with ether, and air-dried.

$[Fe(phen)_3](PF_6)_2$. Three equivalents of phen were added to an aqueous solution of $FeSO_4 \cdot 7H_2O$. The resulting red solution was then filtered into an aqueous solution of NH_4PF_6, precipitating the complex, which was then recrystallized from acetone/ether, washed with ether, and air-dried.

$[Ru(phen)_3](PF_6)_2$. The complex was prepared as described by Kratochvil and Zatko[2] and recrystallized three times from acetone/ether.

Cyclic voltammetry and UV–vis spectroscopy were used to confirm the identity and purity of all the complexes.

Procedure. The experimental procedures for the electrochemical studies in liquid SO_2 have been reported previously.[1,3] The working electrode was a Pt disk (0.046 cm^2) sealed in glass. All potentials are reported vs. an Ag quasi-reference electrode (AgRE), which has a potential equivalent to 0.30 ±0.01 V vs. SCE.[3]

Visible absorption and Resonance Raman data in liquid SO_2 were obtained with a 1.0-cm quartz cuvette encased in a Dewar (Figure 1) similar to the design of Nakane et al.[4] The $Os(bpy)_3^{3+}/SO_2$ solution was prepared by adding $[Os(bpy)_3](PF_6)_3$ to the cell, placing it on the vacuum line, and distilling over SO_2. $[Os(bpy)_3](PF_6)_3$ was prepared by chemically oxidizing $[Os(bpy)_3](PF_6)_2$ in a 20/80 $MeCN/H_2O$ solution with Cl_2. The PF_6^- salt was obtained by reducing the solution volume by half and adding an excess of NH_4PF_6. The spectrum of $Os(bpy)_3^{4+}$ was obtained by transferring an electrochemically generated solution from the electrochemical cell to the absorption cell using 18-gauge Teflon tubing, septum caps, and standard Schlenk-line techniques.[5]

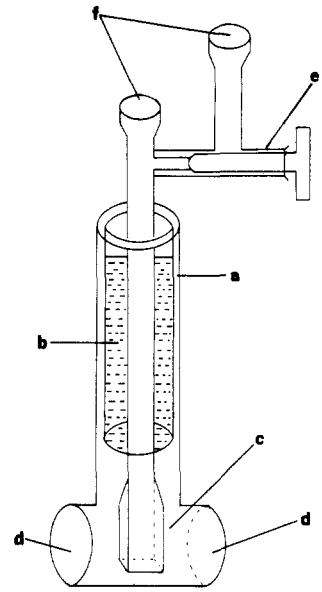

Figure 1. Cell used for visible absorption and Raman spectra at low temperatures: (a) double-walled Pyrex Dewar; (b) cooling agent, dry ice/isopropyl alcohol mixture; (c) 1 × 1 cm quartz cuvette; (d) quartz windows (attached with torr seal epoxy cement); (e) threaded Teflon needle valve vacuum stopcock; (f) standard taper 12/18 female grounded glass joints for attachment to vacuum line and/or electrochemical cell.

NMR samples of $Os(bpy)_3^{2+}$ and $Os(bpy)_3^{3+}$ were prepared by condensing SO_2 directly into an NMR tube containing the complex and $(TMA)BF_4$ and then sealing them off. The solution of the 4+ complex was electrochemically generated and then transferred, by using standard Schlenk-line techniques. $(TMA)BF_4$ was used as both the supporting electrolyte and NMR reference. The $Os(bpy)_3^{4+}$ sample was kept at 77 K prior to obtaining the spectra to decrease the extent of decomposition.

Magnetic susceptibility measurements were carried out by the NMR method of Evans,[6] corrected for the superconducting magnet,[7] by using the shift in the single resonance line of $(TMA)BF_4$.

Resonance Raman spectra were obtained with a SPEX Ramalog EU spectrometer with RCA C31034A photomultiplier, an ORTEC 9300 series photon counter, and a Nicolet 1180 E Raman data system. Laser excitation was provided by a Spectra-Physics 171-18 Ar^+ laser or a Spectra-Physics 171-01 Kr^+ laser. Scattered light was collected in 135° back-scattering geometry through the window of the absorption cell, for the experiments performed in liquid SO_2 ($Os(bpy)_3^{4+}$ and $Os(bpy)_3^{3+}$). In addition, $Os(bpy)_3^{3+}$ was produced and examined in aqueous HCl, with ceric ammonium sulfate present as an oxidant. The RR spectra of $Os(bpy)_3^{2+}$ were examined in aqueous solution. The Os(II), Os(III), and Os(IV) complexes were observed by using laser excitation at 514.5, 457.9, and 356.4 nm. Spectra of $Os(bpy)_3^{4+}$

(2) Kratochvil, B.; Zatko, D. A. *Anal. Chem.* **1964**, *36*, 527–532.
(3) Tinker, L. A.; Bard, A. J. *J. Am. Chem. Soc.* **1979**, *101*, 2316–2319.
(4) Nakane, R.; Watanabe, T.; Kurihara, O.; Oyama, T. *Bull. Chem. Soc. Jpn.* **1963**, *36*, 1376–1381.
(5) Shriner, D. F. "The Manipulation of Air-Sensitive Compounds"; McGraw-Hill: New York, 1969.
(6) Evans, D. F. *J. Chem. Soc.* **1959**, 2003–2005.
(7) Live, D. H.; Chan, S. I. *Anal. Chem.* **1970**, *42*, 791–792.

Table II. Anodic Peak Potentials and Diffusion Coefficients for 2,2′-Bipyridine and 1,10-Phenanthroline Complexes in Liquid Sulfur Dioxide[a]

complex	E_{pa}, V	diffusion coeff ($\times 10^6$) cm^2/s	complex	E_{pa}, V	diffusion coeff ($\times 10^6$), cm^2/s
$Os(bpy)_3^{2+}$	0.55	2.2	$Ru(bpy)_3^{3+}$	2.78[b]	
$Os(bpy)_3^{3+}$	2.16	1.9	$Ru(phen)_3^{2+}$	1.03	1.5
$Os(bpy)_3^{4+}$	3.41	1.8	$Ru(phen)_3^{3+}$	2.60	1.4
$Os(phen)_3^{2+}$	0.58	1.4	$Fe(bpy)_3^{2+}$	0.76[b]	2.0[b]
$Os(phen)_3^{3+}$	2.08	1.2	$Fe(bpy)_3^{3+}$	2.83[b]	
$Os(phen)_3^{4+}$	2.90	1.2	$Fe(phen)_3^{2+}$	0.89	1.6
$Ru(bpy)_3^{2+}$	1.03[b]	2.8[b]	$Fe(phen)_3^{3+}$	2.64	1.5

[a] At −40 °C; 0.1 M $(TBA)BF_4$ as supporting electrolyte. [b] Reference 1.

in frozen SO_2 at 50 K were obtained with use of an Air Products Displex cryostat with a tip machined to accommodate Raman capillary scattering geometry.

Results and Discussion

$[Os(bpy)_3](PF_6)_2$. A typical cyclic voltammogram for the oxidation of $Os(bpy)_3^{2+}$ at −40 °C in liquid SO_2 is shown in Figure 2a. The cyclic voltammetric characteristics of the first two waves are listed in Table I. The data correspond to successive Nernstian one-electron oxidation waves to yield the 3+ and 4+ species:

$$Os(bpy)_3^{2+} \rightleftarrows Os(bpy)_3^{3+} + e^- \qquad E_{pa1} = 0.55\ V \quad (1)$$

$$Os(bpy)_3^{3+} \rightleftarrows Os(bpy)_3^{4+} + e^- \qquad E_{pa2} = 2.16\ V \quad (2)$$

These waves show the following characteristics: anodic and cathodic peak potentials (E_{pa} and E_{pc}) invariant with scan rate (v) (for v between 10 and 200 mV/s) and ΔE_p ($=E_{pa} - E_{pc}$) 46 ± 2 mV (this corresponds closely to the theoretical value of 44 mV for a Nernstian one-electron wave at −40 °C). The third wave observed at $E_{pa3} = 3.41$ V is ~7 times larger than the first two and probably represents a multielectron oxidation followed by a fast chemical reaction, since no reduction current is observed upon potential reversal, even at scan rates as high as 50 V/s.

Controlled-potential coulometry (CPC) carried out at 1.00 V to generate the $Os(bpy)_3^{3+}$ species gave an n_{app} value (faradays per mole of reactant consumed) of 0.99. The dark red solution was stable for at least 6 h at temperatures as high as −15 °C. Coulometric oxidation of the $Os(bpy)_3^{3+}$ solution at 2.40 V and −40 °C produced an orange-red solution. The current during coulometry did not decay to background levels but, after 1.02 times the number of coulombs needed for a one-electron process were passed, reached a constant value that was more than 40 times the background level (and about 4% of the initial current).[8] Voltammetric measurements carried out on this solution (Figure 2b) showed two Nernstian reduction waves at potentials corresponding to those observed for the original oxidations. The magnitudes of these reduction waves were approximately the same as the oxidation waves observed in the original solution. After 1 h, coulometric reduction at 1.00 V to regenerate the $Os(bpy)_3^{3+}$ species yielded only 89% of the total number of coulombs passed during the oxidation. Cyclic voltammetric studies on this $Os(bpy)_3^{3+}$ solution showed that the concentration of the complex had not changed during coulometry, since the peak currents for the $Os(bpy)_3^{3+/4+}$ and $Os(bpy)_3^{2+/3+}$ couples showed their original heights. This behavior is characteristic of a catalytic electrode reaction sequence (EC′)[9] in which the electrogenerated Os-

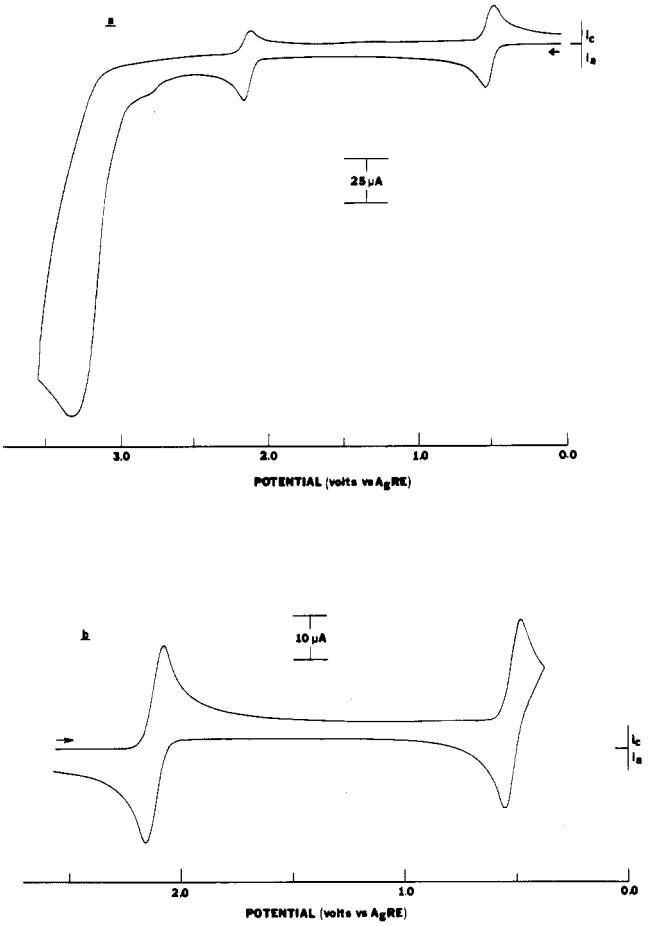

Figure 2. Cyclic voltammograms of (a) 2.98 mM $Os(bpy)_3^{2+}$ in liquid SO_2/0.1 M $(TBA)BF_4$ at −40 °C (scan rate 200 mV/s) and (b) same solution under identical conditions after coulometry oxidation at 2.40 V to form the 4+ species.

$(bpy)_3^{4+}$ species reacts with a nonelectroactive material to regenerate $Os(bpy)_3^{3+}$. Similar behavior was observed with $Ru(bpy)_3^{4+}$ and $Fe(bpy)_3^{4+}$ in liquid SO_2 where the 4+ complexes are believed to react with the solvent to regenerate the 3+ form.[1]

By comparing the steady-state current (i_{ss}) and the initial current (i_0) from the CPC experiments, the pseudo-first-order rate constant for the catalytic reaction can be found. The value of i_{ss} is given by eq 3,[9] where k' is the pseudo-first-order rate

$$\frac{i_{ss}}{i_0} = \frac{k'V/m_0A}{1 + (k'V/m_0A)} \quad (3)$$

constant (s^{-1}), V is the volume of the solution (cm^3), m_0 is the mass-transfer constant (cm/s), and A is the electrode area (cm^2). The values for i_{ss} and i_0 were measured directly from the i vs. t decay curves while the value for the combined constant m_0A was calculated from i_0, C^*, and eq 4, where

$$i_0 = nFAm_0C^*(0) \quad (4)$$

$C^*(0)$ is the bulk concentration of the solution at $t = 0$ s (i.e., the initial bulk concentration) in mol/cm^3 and n and F have their usual significance. The value of k' is $9 \times 10^{-5}\ s^{-1}$ at −40 °C. Thus, $Os(bpy)_3^{4+}$ is at least 3 orders of magnitude less reactive than the analogous Ru and Fe bpy species.[1] The $Os(bpy)_3^{4+}$ species generated at −70 °C is stable for at least 3 h, allowing characterization by cyclic voltammetry and NMR and Resonance Raman spectroscopy.

(8) The background currents observed for the CPC experiments are usually <0.1% of the initial current. The steady-state current reported here and elsewhere are those observed above the background level.

(9) Bard, A. J.; Santhanam, K. S. V. *Electroanal. Chem.* **1970**, *4*, Chapter 3.

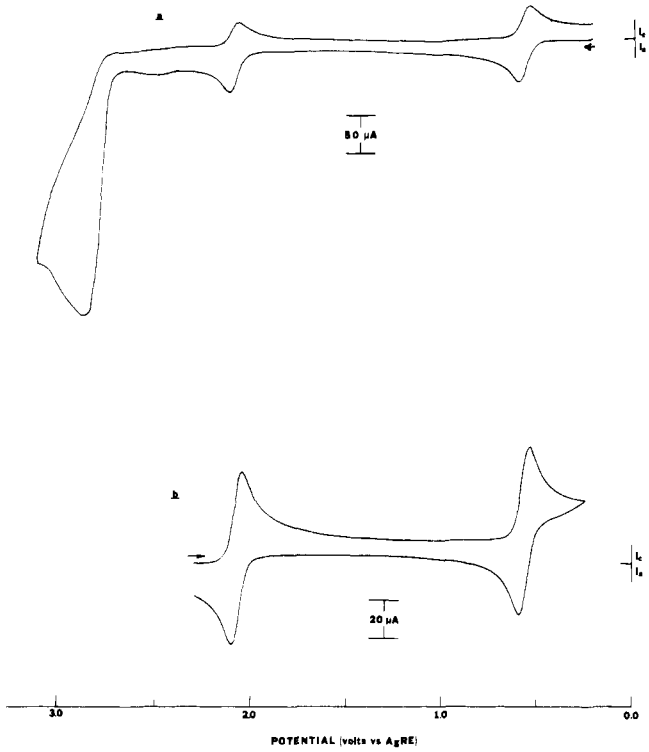

Figure 3. Cyclic voltammograms of (a) 6.91 mM $Os(phen)_3^{2+}$ in liquid SO_2/0.1 M $(TBA)BF_4$ at −40 °C (scan rate 200 mV/s) and (b) same solution under identical conditions after coulometry to form the 4+ species.

$Os(phen)_3(PF_6)_2$. A typical cyclic voltammogram for the oxidation of $Os(phen)_3^{2+}$ in liquid SO_2 at −40 °C is shown in Figure 3a; the behavior is analogous to that of the $Os(bpy)_3^{2+}$ species. The first two oxidation waves correspond to successive Nernstian one-electron oxidations:

$$Os(phen)_3^{2+} \rightleftarrows Os(phen)_3^{3+} + e^- \qquad E_{pa1} = 0.58 \text{ V} \quad (5)$$

$$Os(phen)_3^{3+} \rightleftarrows Os(phen)_3^{4+} + e^- \qquad E_{pa2} = 2.08 \text{ V} \quad (6)$$

Again, E_{pa} and E_{pc} are invariant with scan rate and ΔE_p is 42 ± 2 mV. Cyclic voltammetric data for the two couples are listed in Table I. The third oxidation wave, $E_{pa3} = 2.90$ V, is ~6.5 times larger than the first two, again probably representing an overall multielectron oxidation followed by a fast chemical reaction. No reduction wave is observed upon potential reversal, even at scan rates as high as 50 V/s.

Controlled-potential coulometry carried out at 1.00 V gave a dark red solution and an n_{app} value of 0.99. The resulting $Os(phen)_3^{3+}$ solution was stable for at least 6 h at −40 °C. Coulometric oxidation carried out at 2.30 V gave a dark green solution of $Os(phen)_3^{4+}$. As with the $Os(bpy)_3^{4+}$ species, the current during coulometry did not decay to the background level but, after 1.02 times the number of coulombs needed for a one-electron oxidation were passed, reached a steady-state value that was 2% of the initial current. The 4+ species is again involved in a catalytic reaction, probably with the solvent, to regenerate $Os(phen)_3^{3+}$. When the initial and steady-state currents from the CPC experiment are compared, a rate constant of 6×10^{-5} s^{-1} was calculated for the pseudo-first-order reaction at −40 °C. The solution was, however, sufficiently stable to characterize by cyclic voltammetry (see Figure 3b). At −70 °C the current during coulometry decayed to the background level and an n_{app} value of 0.98 was obtained. The resulting $Os(phen)_3^{4+}$ solution was stable for at least 1 h.

$Ru(phen)_3(PF_6)_2$. The behavior of the second oxidation wave, 3+ → 4+, for $Ru(phen)_3^{2+}$ is very different from that observed for $Os(phen)_3^{2+}$. A typical cyclic voltammogram for the oxidation of $Ru(phen)_3^{2+}$ in liquid SO_2 between 0.00 and 1.50 V (Figure 4b) shows a single wave at $E_{pa} = 1.03$ V corresponding to a Nernstian one-electron oxidation. When the potential was scanned to 2.80 V, a second large oxidation wave was observed at $E_{pa} = 2.60$ V. Successive scans between 0.00 and 2.80 are shown in Figure 4c,d. The third scan shows that the 2+/3+ wave had shifted to more positive potentials and decreased in size; the second oxidation wave also decreased in size. After 10 scans the voltammograms showed a constant shape given in Figure 4e. Additional scans caused the large wave at 1.32 V to increase in height and become narrower and more symmetrical, while the other wave remained unchanged. This behavior is characteristic of a solution species undergoing a redox process and then forming a layer on the electrode. Wave 1 in Figure 4e is probably due to $Ru(phen)_3^{2+}$ in solution, since its potential and shape are the same as those observed in Figure 4b. Wave 2 is due to the layer, probably a polymeric one, since its height increased with successive scans and its shape is characteristics of thin-film behavior. Wave 3 at 2.60 V is again probably due to oxidation of solution species, since its size and diffusional shape are similar to that of wave 1. After about 150 cycles, the electrode was taken out of the liquid SO_2 solution, allowing any adhering solvent to evaporate, and placed in a 0.1 M $(TBA)BF_4$/MeCN solution. The oxidation wave observed in the cyclic voltammogram at $E_{pa} = 1.49$ V vs. SSCE demonstrates the presence of an adherent layer on the electrode surface (Figure 5). The wave shows thin-film behavior, i.e., the peak current is pro-

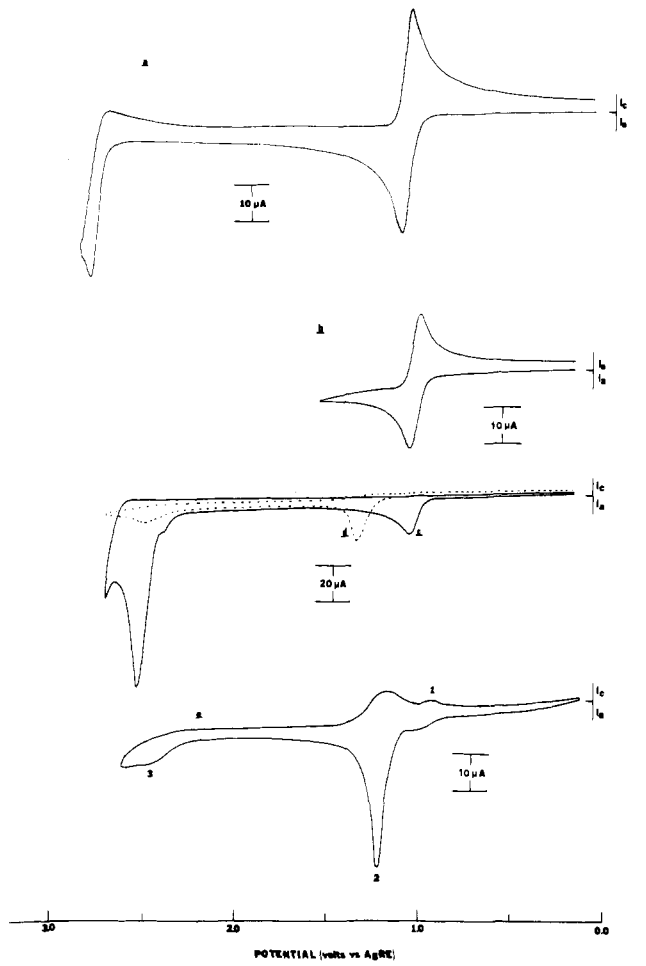

Figure 4. Cyclic voltammograms of $Ru(bpy)_3^{2+}$ and $Ru(phen)_3^{2+}$ in liquid SO_2/0.1 M $(TBA)BF_4$ at −40 °C (scan rate 200 mV/s): (a) scan of 4.70 mM $Ru(bpy)_3^{2+}$; (b) scan of 2.61 mM $Ru(phen)_3^{2+}$ scanned between 0.00 and 1.50 V; (c) first scan of $Ru(phen)_3^{2+}$ between 0.00 and 2.80 V; (d) third scan of $Ru(phen)_3^{2+}$ between 0.00 and 2.80 V; (e) constant shape obtained after 10 scans for $Ru(phen)_3^{2+}$.

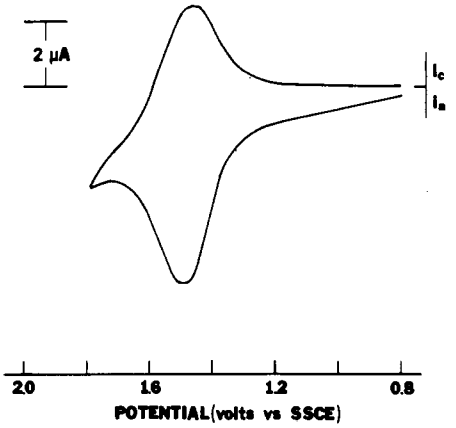

Figure 5. Cyclic voltammogram of the $Ru(phen)_3^{2+}$ polymer in a 0.1 M $(TBA)BF_4/CH_3CN$ solution (scan rate 50 mV/s).

portional to scan rate from 1 to 100 mV/s and ΔE_p is small, 20 mV. However, the width at half-height was 190 mV, approximately twice the expected value.[10] The layer was slightly soluble in MeCN. After 4 min of continual scanning between 0.80 and 1.80 V at 100 mV/s, the anodic peak current was only 90% its original value. If the potential was stepped up from 0.80 to 1.80 V and held there for 2 min, again 10% of the layer was lost. The oxidized form of the polymer seems to be more soluble, since the polymer in the reduced form could be left in a MeCN solution overnight with no apparent loss.

$Fe(phen)_3(PF_6)_2$. The voltammetric behavior of $Fe(phen)_3^{2+}$ in liquid SO_2 was very similar to that observed for $Ru(phen)_3^{2+}$. When the potential was scanned between 0.00 and 1.30 V, a reversible one-electron wave was observed, E_{pa} = 0.89 V, corresponding to the $Fe(phen)_3^{2+/3+}$ couple. If the potential was scanned out to 2.80 V, a large irreversible oxidation wave ~6.5 times larger than the first occurred at E_{pa} = 2.64 V. Additional scans between 0.00 and 2.80 V gave results similar to those of the $Ru(phen)_3^{2+}$ complex. A layer formed that exhibited an oxidation wave at E_{pa} = 1.29 V vs. SSCE in MeCN. As with the $Ru(phen)_3^{2+}$ layer, the peak current was proportional to scan rate, ΔE_p was 20 mV, and the width at half-height was 190 mV. The solubility properties were also similar to those of the Ru polymer.

The electrochemical behavior can be interpreted as the 3+ → 4+ oxidation being ligand centered in the Ru and Fe complexes and being metal centered in the Os species. As shown below, this interpretation is consistent with ^1H NMR results and the molecular orbital model of these species. We have proposed previously[1] that the oxidation of the 3+ bpy complexes of Ru and Fe were ligand centered. This proposal was based on the observation that both oxidation waves occurred at nearly (within 40 mV) the same potential and could be correlated to the visible absorption spectra of the 3+ species and the potential for the 2+/3+ waves.

The oxidation of $Ru(phen)_3^{3+}$ and $Fe(phen)_3^{3+}$ occurs in an overall irreversible multielectron process with i_{pa} ~ 6–7 times that of the Nernstian 2+ → 3+ wave. The potentials for the oxidation of these 3+ phen species also are nearly the same (Table I). Note that the potentials for reduction of the 2+ complexes of Ru and Fe (as well as Os) with bpy and phen in DMF and MeCN are nearly the same (within 80 mV).[11,12] These reductions have been described as ligand centered.[13,14] The observed formation of a polymer layer on the electrode surface from the oxidation of the phen species of Fe and Ru also suggests ligand-centered oxidation, since removal of a metal-centered electron would probably not initiate polymerization.

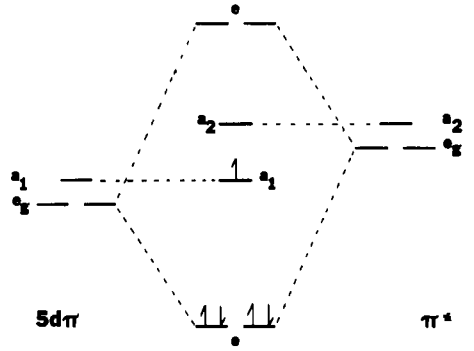

Figure 6. MO diagram for the interaction of the lower 5d orbitals of the metal with the π^* orbitals of the ligand in D_3 symmetry for 3+ species.

Table III. NMR Spectral Data for Osmium 2,2′-Bipyridine Complexes in Liquid Sulfur Dioxide[a]

	chem shift, ppm				coupling const, Hz		
complex	H(3,3′)	H(4,4′)	H(6,6′)	H(5,5′)	J_{34}	J_{45}	J_{56}
$Os(bpy)_3^{2+}$	5.27	4.66	4.52	4.13	7.9	7.5	5.0
$Os(bpy)_3^{3+}$	17.7	4.0	3.6				
$Os(bpy)_3^{4+}$	5.41	5.2	4.92	4.56	8.0	7.5	5.7

[a] At −60 °C; chemical shifts were measured and are reported downfield from $(TMA)BF_4$.

In contrast to the Ru and Fe complexes, oxidation of $Os(phen)_3^{3+}$ does not lead to polymerization. Moreover, the redox potential of the 3+/4+ Os couple lies at less positive potentials by almost 600 mV for both the bpy and phen complexes. This suggests a metal-centered oxidation. (To gain additional information on the electronic distribution of the 4+ species, magnetic susceptibility, ^1H NMR, and Resonance Raman measurements were undertaken.) Note that the further oxidation of $Os(phen)_3^{4+}$ occurs in a wave 6.5 times larger than the peak current for the 2+/3+ couple, suggesting that with Os this oxidation involves a multielectron oxidation of the ligands.

NMR and Magnetic Susceptibility. The oxidation process occurring in the Os complexes can best be described by a molecular orbital diagram. Both the bpy and phen complexes are low spin with D_3 symmetry. A MO diagram based on the work of Hanazaki and Nagakura[15] for the lower oxidation states of bpy complexes is shown in Figure 6. According to the diagram, the 3+ species should be paramagnetic since there is a single electron in the a_1 orbital. Magnetic susceptibility measurements on $Os(bpy)_3^{3+}$ confirm this, with a spin-only magnetic moment of 1.40 μ_B ($\chi_m^{uncor} = 8.16 \times 10^{-4}$ M^{-1} cgsu; diamagnetic correction 3.15×10^{-4} M^{-1}); the 4+ species was diamagnetic.

Additional evidence supporting metal-centered oxidation was obtained from the ^1H NMR analysis of the 2+, 3+, and 4+ species. Figure 7a is the ^1H NMR spectrum of $Os(bpy)_3^{2+}$ in liquid SO_2. The spectrum contains two doublets and two triplets arising from first-order coupling with adjacent protons. The resonances can be assigned on the basis of splitting and coupling constants. Assignments and coupling constants, given in Figure 7a and Table III, are similar to those reported for $Ru(bpy)_3^{2+}$ in Me_2SO.[16] The downfield position of the 3,3′

(10) Hubbard, A. T.; Anson, F. C. *Electroanal. Chem.* **1970**, *4*, Chapter 2.
(11) Saji, T.; Aoyagui, S. *J. Electroanal. Chem. Interfacial Electrochem.* **1975**, *63*, 31–37.
(12) Gaudiello, J., unpublished results.
(13) Saji, T.; Aoyagui, S. *J. Electroanal. Chem. Interfacial Electrochem.* **1975**, *58*, 401–410.
(14) Creutz, C. *Comments Inorg. Chem.*, in press.
(15) Hanazaki, I.; Nagakura, S. *Bull. Chem. Soc. Jpn.* **1971**, *44*, 2312.
(16) Lytle, F. E.; Petrosky, L. M.; Carlson, L. R. *Anal. Chim. Acta* **1971**, *57*, 239–247.

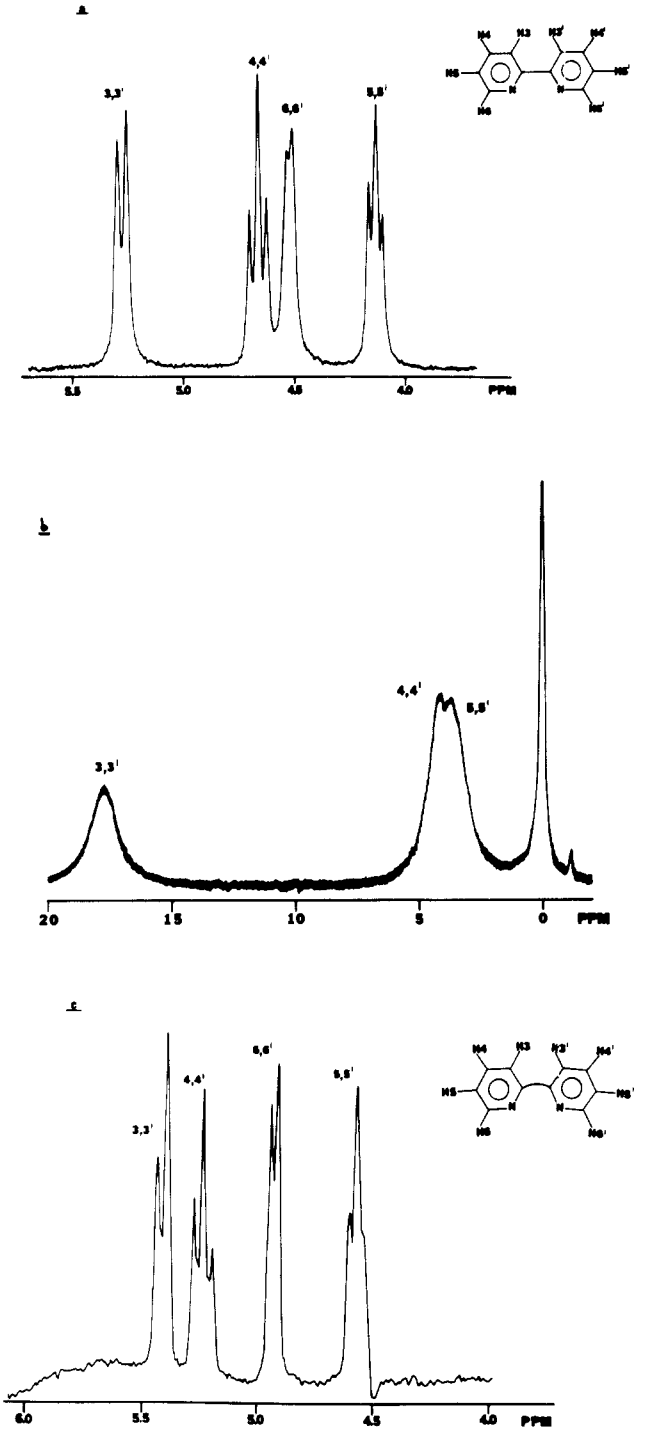

Figure 7. ^{1}H NMR spectra of $Os(bpy)_3^{n+}$ in liquid SO_2 at −60 °C: (a) $Os(bpy)_3^{2+}$; (b) $Os(bpy)_3^{3+}$; (c) $Os(bpy)_3^{4+}$.

protons relative to the others can be attributed to van der Waals deshielding interactions caused by forcing of the 3,3′ protons together when the ligand bonds to the metal. Similar behavior has been observed with $Ru(bpy)_3^{2+}$,[16] $Fe(bpy)_3^{2+}$,[17] and $Os(4,4'\text{-}Me_2bpy)_3^{2+}$.[18]

The ^{1}H NMR spectrum of $Os(bpy)_3^{3+}$ (Figure 7b) is similar to that obtained by DeSimone and Drago in MeCN.[19] The broad resonances occurring over a large range is characteristic of a paramagnetic compound. The peak at 17.2 ppm has been assigned to the 3,3′ protons while the peaks at 4.0 and 3.6 ppm

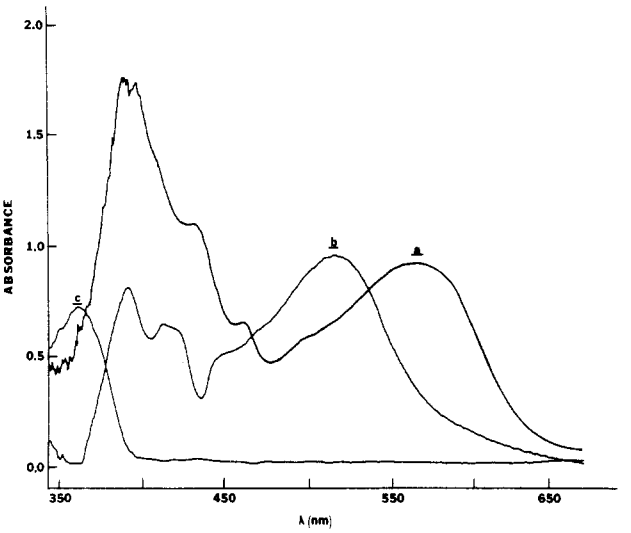

Figure 8. Absorption spectra of $Os(bpy)_3^{3+}$ and $Os(bpy)_3^{4+}$ in liquid SO_2 (path length 1 cm): (a) 1.53×10^{-3} M $Os(bpy)_3^{4+}$; (b) 2.40×10^{-3} M $Os(bpy)_3^{4+}$; (c) liquid SO_2.

Table IV. Summary of Spectra Data for $Os(bpy)_3^{3+}$ and $Os(bpy)_3^{4+}$ in Liquid Sulfur Dioxide

complex	abs peak, nm	ϵ, M^{-1} cm^{-1}	complex	abs peak, nm	ϵ, M^{-1} cm^{-1}
$Os(bpy)_3^{3+}$	567	590	$Os(bpy)_3^{4+}$	515	392
	462	~150		413	~120
	432	~200		393[a]	~150[a]

[a] May be in error due to the large absorption of SO_2 in this region.

are due to the 4,4′ and 5,5′ protons, respectively. Drago also observed a very broad singlet from the 6,6′ protons at ca. −27 ppm, which we could not observe due to instrumental limitations.

The spectrum of the $Os(bpy)_3^{4+}$ complex is shown in Figure 7c. Its position and appearance are similar to that of the 2+ species. Two doublets and two triplets are observed, although the triplet at 4.6 ppm is not well-defined. Its integrated area, however, is the same as the other three. Peak assignments are again based on splitting and coupling constants and are listed in Table III. The values obtained are very close to those observed for $Os(bpy)_3^{2+}$. There are, however, two main differences between the 2+ and 4+ spectra. The resonances for the 4+ species are shifted downfield relative to the 2+ species, and the position of the 3,3′ peak is now close to those observed for the other protons.

The downfield shift upon oxidation may be due to an inductive effect; the higher charge on the metal will decrease the electron density at each carbon atom. The higher metal charge would also lead to a shorter Os–N bond length, causing the rings to become drawn in and forcing the protons at the 3,3′ positions apart (see Figure 7c). This would remove some of the van der Waals deshielding interaction, causing these resonances to remain with the others.

Visible Absorption Spectra. The visible absorption spectra of $Os(bpy)_3^{3+}$ and $Os(bpy)_3^{4+}$ in liquid SO_2, along with SO_2 itself, are shown in Figure 8. Spectroscopic data for the two complexes are summarized in Table IV. The shorter wavelength portion of the spectra for the Os complexes are distorted by the absorption band of SO_2. The 3+ spectrum (Figure 8a) is similar in shape and intensity to that previously reported in 3 N HCl.[20] The broad band at 567 nm has been assigned

(17) Castellano, S.; Gunther, H.; Ebersole, S. *J. Phys. Chem.* **1965**, *69*, 4166–4176.
(18) Bryant, G. M.; Fergusson, J. E. *Aust. J. Chem.* **1971**, *24*, 441–444.
(19) DeSimone, R. E.; Drago, R. S. *J. Am. Chem. Soc.* **1970**, *92*, 2343–2352.
(20) Bryant, G. M.; Fergusson, J. E.; Powell, H. K. J. *Aust. J. Chem.* **1971**, *24*, 275–286.

Table V. Resonance Raman Frequencies of $Os(bpy)_3^{n+}$ Complexes (cm^{-1})

$Os(bpy)_3^{2+}$ [a]	$Os(bpy)_3^{3+}$ [b]	$Os(bpy)_3^{4+}$ [c]
1610	1610	1611
1557	1567	1563
		1512
1489	1502	1492
		1459
		1432
1323	1324	masked by SO_2
1273	1280	1288
		1250
1180	1168	
	1158	
	1114	1121
		1078
1051	masked by HSO_4^-	1050
1031	masked by HSO_4^-	1038
	masked by HSO_4^-	1016

[a] 300 K; H_2O. [b] 300 K; 1 M HCl/H_2O. [c] 50 K; frozen SO_2.

to a ligand-to-metal charge transfer. The lower intensity bands at 462 and 432 nm are thought to be vibrational structures.[20]

The spectrum of $Os(bpy)_3^{4+}$ contains a broad band at 515 nm along with two shoulders at 413 and 393 nm. The absorption at 515 nm allows the use of the 514.5-nm line of the Ar^+ laser to obtain the resonance Raman spectra of the $Os(bpy)_3^{4+}$ species. These results are discussed below.

Resonance Raman Studies of $Os(bpy)_3^{n+}$. Figure 9 shows the RR spectra of $Os(bpy)_3^{2+}$, $Os(bpy)_3^{3+}$, and $Os(bpy)_3^{4+}$. The spectrum of the 4+ complex exhibits two prominent peaks due to the SO_2 solvent, and the 3+ spectrum shows a strong peak due to HSO_4^- in the 1 M HCl solution containing sulfate ion as an intensity reference. The spectra of the 4+ complex are shown both in liquid SO_2 and in frozen SO_2 (50 K). The observed RR frequencies of the $Os(bpy)_3^{n+}$ complexes between 1000 and 1700 cm^{-1} are given in Table V.

Typically, RR spectra of $M(bpy)_3^{n+}$ complexes exhibit seven relatively intense peaks in the 1000–1700-cm^{-1} region.[21,22] To a good approximation, these correspond to the seven symmetric in-plane C–C and C–N stretches expected of the bipyridine ligand in D_3 symmetry. Other symmetric modes in this frequency region include the four in-plane C–H wags, and these are sometimes observed as weak features.[21] Lower effective symmetry, which results in inequivalency of the rings within a bpy ligand, may result in more complex RR spectra,[23] as may inequivalency of entire bpy structures due to, for example, formation of a ligand radical.[22] The "typical" bpy spectrum is particularly characteristic of the five modes above 1200 cm^{-1}, unless ligand inequivalency or symmetry-breaking perturbations occur.

It can be seen from Figure 9 and Table V that both the Os(II) and Os(III) complexes exhibit the typical RR spectra of bpy complexes. Comparable RR modes are at uniformly higher frequency in the Os(III) complexes than in Os(II), reflecting diminished effectiveness of the Os(III) oxidation state as an electron donor to the bpy π^* orbitals. The RR spectrum of $Os(bpy)_3^{4+}$ is anomalously complex. Thirteen rather than seven RR modes appear between 1000 and 1700 cm^{-1}, and eight rather than five appear between 1200 and 1700 cm^{-1}. In addition, there is good evidence that one or two $Os(bpy)_3^{4+}$ modes are obscured by the SO_2 peak at 1334 cm^{-1}. Clearly, this complex has too many RR-active modes for the simple D_3 model to be valid, even if all the possible C–H motions are included.

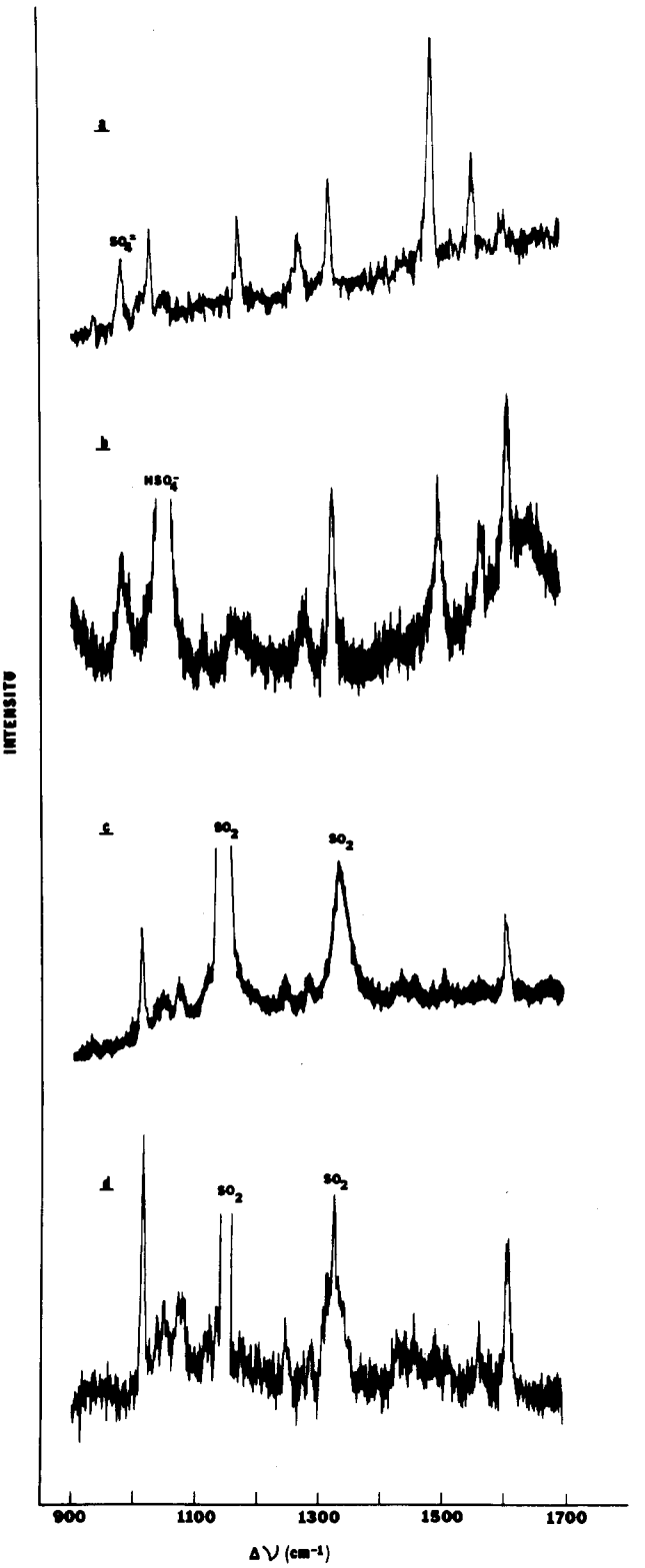

Figure 9. Resonance Raman spectra of $Os(bpy)_3^{n+}$ complexes: (a) $Os(bpy)_3^{2+}$ in H_2O, SO_4^{2-} added as an internal reference, 514.5-nm excitation; (b) $Os(bpy)_3^{3+}$ in 1 M HCl/ceric ammonium sulfate solution, 514.5-nm excitation; (c) $Os(bpy)_3^{4+}$ in liquid SO_2/0.10 M $(TBA)BF_4$ at ca. −40 °C, 514.5-nm excitation; (d) $Os(bpy)_3^{4+}$ in frozen SO_2/0.10 M $(TBA)BF_4$ at ca. 50 K, 514.5-nm excitation.

The $Os(bpy)_3^{4+}$ spectrum could be rationalized in terms of an $Os^{III}(bpy)_2(bpy^{+\cdot})^{4+}$ formulation for the "Os(IV)" oxidation state. In this scenario, the neutral bpy ligands and the oxidized bpy radical cation contribute overlapping peak patterns to the

(21) Clark, R. J. H.; Turtle, P. C.; Strummen, D. P.; Streusand, B.; Kincaid, J.; Nakamoto, K. *Inorg. Chem.* **1977**, *16*, 84–89.
(22) Bradley, P. G.; Kress, N.; Hornberger, B. A.; Dallinger, R. F.; Woodruff, W. H. *J. Am. Chem. Soc.* **1981**, *103*, 7441–7446.
(23) Chisholm, M. H.; Huffman, J. C.; Ruthwell, I. P.; Bradley, P. G.; Kress, N.; Woodruff, W. H. *J. Am. Chem. Soc.* **1981**, *103*, 4945–4947.

observed RR spectra, with the $bpy^{+\cdot}$ frequencies uniformly lowered by removal of a bonding electron. Such a situation occurs, for example, in the MLCT state of $Ru(bpy)_3^{2+}$, which may be formulated realistically as $Ru^{III}(bpy)_2(bpy^{-\cdot})^{2+}$.[22] In the present case, however, such an interpretation is apparently precluded by the other evidence cited herein concerning the Os(IV) oxidation state; we must understand the complexity of the RR spectrum in other terms.

The electronic configuration at the 5d orbitals of Os(IV) in octahedral microsymmetry is $t_{2g}^4e_g^0$. The four-electron-occupied t_{2g} set is triply degenerate and, accordingly, may experience Jahn–Teller splitting. Greatest energetic stabilization is obtained if the splitting is as shown in Figure 6 (for Os(III)), giving a fully occupied lower energy subset of orbitals having e symmetry and vacant a-type orbitals. The observed diamagnetism of $Os(bpy)_3^{4+}$ is consistent with such a splitting pattern and, furthermore, requires that the splitting of the originally t_{2g} orbitals exceed the electronic pairing energy. There are no such energetic requirements upon the magnitude of the splitting in the Os(III) case (Figure 6), because the spin multiplicity at the metal ion is the same ($S = {}^1/_2$) regardless of splitting.

Inasmuch as the t_{2g} orbitals have symmetry with respect to the bpy ligands, splitting of the energies of the metal orbitals and differences in their electronic occupation may lead to inequivalent bond orders among the bpy ligands and even between the two rings of a single bpy. This in turn will be reflected as complexity in the RR spectrum because differing strengths of similar bonds will result in vibrational frequency shifts. Static splitting of such a nature is chemically dictated in $Mo(bpy)_2(i\text{-}PrO)_2(i\text{-}PrO)_2$ (*i*-PrO = isopropoxide) and is reflected in splitting of the RR modes of the bpy ligands in this complex.[23] We note that the electronic configuration of this Mo(II) complex is d^4, as is the case with metal-oxidized $Os(bpy)_3^{4+}$.

In the case of $Os(bpy)_3^{4+}$, there is no chemical or structural feature that dictates which of the split t_{2g} orbitals is higher or lower in energy. Accordingly, the splitting may be dynamic with respect to the directivity of the metal π orbitals that are occupied, and therefore ligand inequivalency may also be dynamic. The NMR spectrum of $Os(bpy)_3^{4+}$ shows no ligand inequivalency (Figure 7), but this result is equally consistent with the absence of inequivalency and with dynamic inequivalency that is rapidly averaged on the NMR time scale. The complex RR spectrum confirms substantial ligand inequivalency. This inequivalency may be "static" on the vibrational time scale as in the case of the MLCT states of $Ru(bpy)_3^{2+}$ and $Os(bpy)_3^{2+}$.[22] To account for some of the frequency splittings observed in $Os(bpy)_3^{4+}$ (Table V), however, a static inequivalency would have to amount virtually to one-electron oxidation of one of the ligands. This is the same as the Os(III)/Os(IV) oxidation being ligand centered, which is contrary to other evidence presented herein. Alternatively, the splitting of the metal t_{2g} orbitals could be dynamic on a time scale approaching that of electronic motions. If this were the case, the ligands would experience a triple-minimum electronic potential. If the potential minima were sufficiently deep, this could split the bpy vibrational levels significantly and account for the observed complexity of the RR spectra of $Os(bpy)_3^{4+}$.

Splitting of the t_{2g} orbitals also occurs in $Os(bpy)_3^{3+}$ and $Ru(bpy)_3^{3+}$. Nevertheless, the RR spectra of these d^5 M(III) complexes appear similar to those of the d^6 M(II) complexes, where no Jahn–Teller splitting can occur. Apparently, the splitting of the t_{2g} orbitals in the d^5 complexes does not represent a symmetry-breaking perturbation with respect to the bpy ligand vibrations.

Conclusions

The electrochemical and spectroscopic data from this and previous work suggest that the oxidation in liquid SO_2 of the 3+ complexes of Ru and Fe with bpy and phen can be represented by

$$M^{III}L_3^{3+} \rightleftarrows M^{III}L_2L^{+\cdot 4+} + e^-$$

(M = Ru, Fe; L = phen, bpy)

while for Os

$$Os^{III}L_3^{3+} \rightleftarrows Os^{IV}L_3^{4+} + e^-$$

The 4+ Ru and Fe phen complexes polymerize to form an electroactive layer on the electrode surface, while the 4+ Os bpy and phen complexes are quite stable.

Acknowledgment. This work was supported by the National Science Foundation (Grant CHE 7903729). The assistance of Jim Willin in obtaining the ^1H NMR spectra and useful discussions on their interpretation by Dr. Ben A. Shoulders are gratefully acknowledged. We also thank William Bruton for constructing the absorption and electrochemical cells and Dr. Hector Abruna for advice on the preparation of the Os complexes.

Registry No. $[Fe(phen)_3](PF_6)_2$, 17112-07-1; $[Ru(phen)_3](PF_6)_2$, 60804-75-3; $[Os(bpy)_3](PF_6)_2$, 75441-79-1; $[Os(phen)_3](PF_6)_2$, 75441-76-8; $Os(bpy)_3^{3+}$, 30032-51-0; $Os(phen)_3^{3+}$, 47837-53-6; $Os(bpy)_3^{4+}$, 87901-16-4; $Os(phen)_3^{4+}$, 87901-17-5; $Ru(bpy)_3^{3+}$, 18955-01-6; $Ru(phen)_3^{3+}$, 23633-32-1; $Fe(bpy)_3^{3+}$, 18661-69-3; $Fe(phen)_3^{3+}$, 13479-49-7; $Ru(bpy)_3^{4+}$, 83207-87-8; $Fe(bpy)_3^{4+}$, 83207-86-7; SO_2, 7446-09-5.